Targeted expression of a dominant-negative N-cadherin in vivo delays peak bone mass and increases adipogenesis

Charlles H. M. Castro[1,3,*], Chan Soo Shin[1,4,*], Joseph P. Stains[1], Su-Li Cheng[1], Sharmin Sheikh[1], Gabriel Mbalaviele[1,5], Vera Lucia Szejnfeld[3] and Roberto Civitelli[1,2,‡]

[1]Division of Bone and Mineral Diseases, Departments of Internal Medicine, and [2]Cell Biology and Physiology, Washington University School of Medicine, 216 S. Kingshighway Blvd, St Louis, MO 63110, USA
[3]Universidade Federal de São Paulo-Escola Paulista de Medicina, Rua Botucatu 740, São Paulo-SP, Brasil
[4]Department of Internal Medicine, Seoul National University College of Medicine, 28 Yongon-Dong, Chongno-Gu, Seoul 110-774, Republic of Korea
[5]Pfizer Incorporated, 700 Chesterfield Parkway West, Chesterfield, MO 63107, USA
*These authors contributed equally to this work
‡Author for correspondence (e-mail: rcivitel@im.wustl.edu)

Summary

We studied the function of osteoblast cadherins in vivo by transgenic expression of a truncated N-cadherin with dominant-negative action, driven by an osteoblast-specific promoter (OG2-NcadΔC). During the first 3 months of life, bone mineral density was reduced, whereas percent body fat was increased in transgenic animals compared with wild-type littermates, with associated decreased bone formation rate and osteoblast number, but normal osteoclast number. Osteoblast differentiation was delayed in calvaria cells isolated from transgenic mice. Likewise, the number of osteoblast precursors in bone marrow stromal cells from OG2-NcadΔC mice was decreased compared with wild-type cultures, whereas the number of adipogenic precursors was increased. In vitro, a transcriptionally active β-catenin mutant reversed the delay in osteoblast differentiation and the exuberant adipogenesis. Thus, in vivo disruption of cadherin function hinders osteoblast differentiation and favors, indirectly, bone marrow progenitor cell commitment to the alternative adipogenic lineage via interference with β-catenin signaling. This results in decreased bone formation, delayed acquisition of peak bone mass and increased body fat.

Key words: Cell-cell adhesion, Mesenchymal differentiation, Cadherins, Adipogenesis, Transgenic mice

Introduction

Cadherins are a family of integral transmembrane proteins that mediate calcium-dependent cell-cell adhesion, a process necessary for cell aggregation and sorting during tissue morphogenesis, and for development and maintenance of cell polarity, cell migration, proliferation and survival (Gumbiner, 1996; Takeichi, 1995). In addition to their role as a structural component of adherens junctions, cadherins can also modulate intracellular signaling. The cytoplasmic domain of cadherins binds to β-catenin and plakoglobin, two vertebrate homologs of *Drosophila* armadillo, which link cadherins to the actin cytoskeleton via α-catenin (Nagafuchi, 2001). Through their association with β-catenin, cadherins can also interfere with the Wnt signaling system, of which β-catenin is an integral component. In this function, β-catenin participates in the formation of a transcriptionally active complex which also includes members of the T-cell factor/lymphoid enhancer factor (Tcf/Lef) family of DNA-binding proteins (Cadigan and Nusse, 1997; Peifer and Polakis, 2000). Cadherin modulation of β-catenin signaling is complex. On the one hand, β-catenin bound to cadherins may represent a readily available pool for nuclear translocation, thus favoring Wnt signaling. On the other hand,

excess binding to cadherin on the cell surface may decrease β-catenin nuclear pools, thus antagonizing Tcf/Lef transactivation (Fagotto et al., 1996; Sadot et al., 1998).

Osteoblasts, bone forming cells, express multiple cadherins, primarily N-cadherin, cadherin-11 and cadherin-4/R-cadherin (Okazaki et al., 1994; Cheng et al., 1998; Ferrari et al., 2000). We and others have previously shown that upregulation of N-cadherin and cadherin-11 defines osteogenic cell differentiation from mesenchymal precursors (Shin et al., 2000; Kawaguchi et al., 2001b), and disruption of cadherin-mediated cell-cell adhesion hinders osteoblast differentiation and bone matrix production (Cheng et al., 1998; Cheng et al., 2000; Ferrari et al., 2000). Importantly, targeted disruption of the cadherin-11 gene results in mild skeletal defects with reduced bone density (Kawaguchi et al., 2001a). This mild skeletal phenotype and the overlapping distribution patterns of N-cadherin and cadherin-11 in the skeletal tissue suggest that N-cadherin may compensate for lack of cadherin-11, and raise the possibility that the two osteoblast cadherins may serve common functions in controlling bone formation (Civitelli et al., 2002). Unfortunately, homozygous loss of the N-cadherin gene results in early embryonic lethality, thus precluding the use of this model for any studies of adult bone (Radice et al., 1997).

We have generated a transgenic mouse line expressing a truncated N-cadherin with dominant-negative action in osteoblasts. This approach allows for non-isotype specific interference with cadherin function, thus overcoming a potential redundancy. The truncated cadherin we used lacks most of the extracellular domain but its cytoplasmic C terminal tail is intact, including the β-catenin binding site, and it has been proven to inhibit cadherin function in vivo (Kintner, 1992; Hermiston and Gordon, 1995) and in osteoblast cultures (Cheng et al., 2000; Ferrari et al., 2000). We found that targeted expression of this dominant-negative cadherin in osteoblasts in vivo reduced bone formation and osteoblast number, leading to a delay in achievement of peak bone mass, while increasing body adiposity. This phenotype is associated with altered lineage allocation of mesenchymal bone marrow precursors, resulting in reduced osteogenesis and increased adipogenesis – an abnormality that in vitro can be reversed by exogenous expression of transcriptionally active β-catenin.

Materials and Methods

Generation of transgenic mice

A 1.3 kb DNA fragment containing the OG2 promoter was excised from pII1.3-Luc, a kind gift of Dr Gerard Karsenty, Baylor College of Medicine, Houston, TX (Ducy and Karsenty, 1995), and ligated into pcDNA3 after digestion with *Nru*I and *Hin*dIII (Invitrogen). This resulted in replacement of the CMV promoter with the OG2 promoter (OG2-pcDNA3). To clone NcadΔC into this vector, two PCR primers were designed to amplify a 850 bp product from pSP72NcadΔC, courtesy of Dr Chris Kintner, Salk Institute, San Diego, CA (Kintner, 1992). The PCR product contains the entire NcadΔC reading frame, an *Eco*RI linker at the 5′ end and a FLAG epitope tag, followed by a stop codon and a *Hin*dIII site. The product was ligated in OG2-pcDNA3, yielding OG2-NcadΔC (Fig. 1A). A 2.9 kb fragment containing the OG2 promoter, NcadΔC, and BGH polyA was excised from OG2-NcadΔC for microinjection into the male pronucleus of fertilized eggs (E0.5), harvested from superovulated, 4-week-old B6C3F1 females. The eggs were implanted into the reproductive tract of 3-5-month-old Swiss Webster pseudopregnant female mice. Twenty-five founder mice from three litters were screened for the expression of the transgene using both PCR primers designed to amplify a sequence encompassing the 3′ end of the OG2 promoter and the 5′ end of NcadΔC; and a cDNA probe hybridizing to the transition region and a small sequence of NcadΔC (Fig. 1A). Hybridization was performed on genomic DNA after digestion with *Pst*I, and transgene-positive founders were identified by a 1.1 kb band in Southern analysis, or a 256 bp PCR product (Fig. 1B). Mice were fed regular chow ad libitum and housed in a room maintained at constant temperature (25°C) on a schedule of 12 hours of light and 12 hours of dark.

Bone mineral density measurements and body composition analysis

Total body bone mineral density and percent body fat were monitored by dual-energy X-ray absorptiometry using a PIXImus scanner (GE/Lunar, Madison, WI). Calibration of the instrument was conducted daily as suggested by the manufacturer. After induction of anesthesia with 100 mg/kg ketamine and 10 mg/kg zylaxine i.p., mice were placed on the imaging-positioning tray in a prostrate position. One investigator (CHMC) performed and analyzed all the scans using the software provided by the manufacturer. Heads were excluded from the analysis by masking. The precision of this technique, assessed by the root mean square method after scanning 17 mice three times with repositioning, was 1.34% for bone mineral density and 3.31% for percent body fat.

Bone histology and histomorphometry

Histomorphometric analysis was performed on tibial metaphyses of 2-month-old mice. Bone samples were dissected out and fixed in 70% ethanol. Samples were left undecalcified, dehydrated, infiltrated and embedded in methyl methacrylate. Longitudinal sections were cut frontally in the proximal tibial metaphysis using a Leica RM 2165 microtome. Four-micrometer sections were stained with Goldner's trichrome technique or for tartrate resistant acid phosphatase activity and counterstained with methyl green and thionin for identification of osteoclasts and osteoblasts (Liu and Kalu, 1990), while 8 µm sections were left unstained for dynamic bone histomorphometry. Quantitative histomorphometry was performed in an area 175-875 µm distal to the growth plate at 200× magnification (dynamic parameters) or 400× magnification (cellular and structural parameters), using the OsteoMeasure software program (Osteometrix, Atlanta, GA), a Nikon Eclipse E400 light/epifluorescent microscope, a CalComp Drawing Board III digitizing tablet and a video subsystem. The width of growth plate was measured by tracing the upper and lower margins of the growth plate at 200× magnification. Following an established nomenclature (Parfitt et al., 1987), the following static parameters of bone remodeling were estimated: trabecular bone volume as a percentage of total tissue volume, trabecular thickness (µm), trabecular number (per mm), trabecular separation (µm), osteoblast perimeter per bone perimeter (percentage), osteoblast number per bone perimeter (per mm), osteoclast perimeter per bone perimeter (percentage), osteoclast number per bone perimeter (per mm) and growth plate width (µm). For assessment of dynamic histomorphometric parameters, 2-month-old mice were labeled twice by injection of calcein (20 mg/kg i.p., Sigma-Aldrich) on days 8 and 3 before killing. After methylmethacrylate embedding, 8 µm thick sections were mounted unstained in Fluoromount (Electron Microscopy Sciences, Fort Washington, PA) for evaluation by fluorescent microscopy and calculation of the following dynamic parameters on two nonconsecutive sections per animal: mineral apposition rate (µm/day; mean distance between two fluorescent labels divided by the number of days between the labels), and bone formation rate/tissue volume (%/year; annual fractional volume of trabecular bone formed/ tissue volume). Results represent the average±s.d. of at least three sections per mice from four transgenic and four wild-type mice.

Cell culture and phenotypic characterization

Calvarial cells (CLVC)

Osteoblast-enriched calvaria cultures were prepared from newborn mice by sequential collagenase digestion as previously described (Lecanda et al., 2000), and grown in alpha modified essential medium (αMEM; Mediatech, Herndon, VA), supplemented with 10% fetal bovine serum (FBS; Atlanta Biologicals, Norcross, GA) and 100 IU/ml penicillin and 100 µg/ml streptomycin (Sigma Chemicals, St Louis, MO). Approximately three to five calvariae were pooled to prepare the cell cultures used in each experiment.

Bone marrow stromal cells (BMSC)

After dissection, the epiphyseal ends of femora and tibiae of 2-3-month-old mice were removed and the marrow cavity of the shafts was flushed with 5 ml of αMEM with penicillin and streptomycin using a 25-gauge needle. The material was then filtered through a 70 µm cell strainer (Falcon). Red blood cells in marrow cells were hemolyzed in 0.017 M Tris-HCl buffer, pH 7.5, containing 0.8% NH_4Cl, and the resulting BMSC suspension was rinsed twice in PBS and plated at $1-2.5×10^5$ cells/cm^2.

Alkaline phosphatase activity

As a marker of osteogenic differentiation, alkaline phosphatase activity was measured in cell extracts according to previously

published and established methods (Lecanda et al., 2000). Enzymatic activity was normalized for total protein content (Bio-Rad protein assay kit) and expressed as nmol of *p*-nitrophenol produced from *p*-nitrophenyl phosphate per minute per mg of protein.

In vitro mineralization

To assess the capacity of osteoblastic cells to mineralize in vitro, CLVC were cultured in the presence of 50 µg/ml ascorbic acid (AA) and 10 mM β-glycerophosphate (β-GP) for 2-3 weeks, and subjected to Von Kossa staining, as previously described (Lecanda et al., 2000).

Adipogenesis assay

For adipogenesis BMSC were seeded at $10^5/cm^2$ in αMEM containing 15% FBS and cultured for 14 days. One-half of the medium was replaced with fresh medium on day 5 and adipogenesis was stimulated by adding 0.5 mM IBMX, 60 µM indomethacin and 0.5 µM hydrocortisone (Sigma-Aldrich, St Louis, MO) on day 11. On day 14, cultures were fixed in 10 mmol/l sodium periodate, 2% paraformaldehyde, 75 mmol/l L-lysine dihydrochloride and 37.5 mmol/l sodium phosphate (dibasic), pH 7.4, for 15 minutes, air dried and stained in a filtered solution of 0.3% Oil Red O in 60% isopropanol for 30 minutes.

Detection and quantification of bone marrow mesenchymal progenitor cells

Limiting dilution analysis (Bellows and Aubin, 1989) was applied to determine the number of bone marrow mesenchymal progenitor cells that were able to produce colony forming units (CFU). BMSC harvested from the femur and tibia of 2-3-month-old mice were diluted in growth medium (αMEM + 15% FBS, 100 IU/ml penicillin and 100 µg/ml streptomycin) and plated at densities ranging between 10^5 and 10^3 cells/well in 96-well plates (corresponding to 3.2×10^4 to 3.2×10^2 cell/cm²). After 1 week in culture, the medium was replaced with fresh growth medium with or without additives, as noted below. To determine the number of CFU-Fibroblasts (CFU-F), the plates were fixed in 100% ethanol after 2 weeks in culture and stained with Giemsa. Wells containing more than 20 Giemsa positive fibroblastoid cells were considered positive for CFU-F. For the CFU-Adipocytes (CFU-A) assay, cells were cultured in the presence of an adipogenic cocktail (0.5 mM IBMX, 60 µM indomethacin, and 0.5 µM hydrocortisone) during the second week. They were fixed and stained as described above (adipogenesis assay), and adipocytes were identified as red, lipid vacuole-containing cells. Wells containing more than 20 red-stained cells were considered positive for CFU-A. To determine the number of CFU-Osteoblasts (CFU-O), cells were cultured for 4 weeks in the presence of a mineralizing medium (50 µg/ml AA and 10 mM β-GP), with weekly medium replacement. After 4 weeks, the wells were stained by the Von Kossa method, as described above, and the number of wells with more than 20 cells having a dark brown extracellular matrix were considered positive for CFU-O. The number of CFUs in each assay and at each dilution was estimated according to the formula, $F_o=e^{-x}$; where F_o is the fraction of colony-negative wells relative to the total number of wells seeded; e=2.71 (base of natural logarithms); and x is the number of CFUs per well (Bellows and Aubin, 1989).

Immunoprecipitation, western analysis and subcellular fractionation

For tissue extracts, calvaria from wild-type or transgenic mice were dissected, rinsed in phosphate-buffered saline, cut into small pieces, and incubated in RIPA buffer (10 mM Tris, pH 8.0; 150 mM NaCl; 1% NP-40; 0.1% sodium dodecyl sulfate and 1% sodium

deoxycholate containing a protease inhibitor cocktail (Sigma)) for 30 minutes at 4°C. Samples were subsequently sonicated on ice, and the insoluble material removed by centrifugation. The protein content of the supernatants was determined using the BCA protein assay (Pierce). The samples (250 µg) were then diluted in 1 ml immunoprecipitation buffer (10 mM Tris, pH 8.0, 150 mM NaCl, 1% NP-40 and 1% BSA). Following pre-clearing of the supernatants with Protein A/G Plus beads (Santa Cruz), the polyclonal antibody PEP.1, which recognizes the C-terminal intracellular tail of *Xenopus* N-cadherin (generous gift of Dr Barry Gumbiner, University of Virginia, Charlottesville, VA), was added and the samples incubated overnight at 4°C with gentle shaking. Protein A/G Plus beads were incubated with the samples for 1 hour, then pelleted by centrifugation. The beads were washed three times in immunoprecipitation buffer, then twice in PBS. Bound material was eluted from the beads by boiling in SDS-PAGE sample buffer. Samples were then electrophoresed on SDS-PAGE gels and examined by immuoblotting with anti-FLAG M2 antibodies (Sigma).

For whole-cell lysates, CLVC grown on 100 cm² Petri dishes were extracted in a buffer containing 50 mM Tris-HCl, pH 7.4, 150 mM NaCl, 20mM EDTA, 1% Triton X-100, 1% sodium deoxycholate, 0.1% SDS and protease inhibitors. Proteins were separated by 10% SDS-PAGE, and electroblotted to a nitrocellulose membrane. For subcellular fractionation of β-catenin, cells were rinsed with cold PBS, scraped from the plate and centrifuged at 10,000 *g* for 5 minutes at 4°C. The pellets were gently resuspended in a hypotonic buffer (10 mM HEPES-KOH, pH 7.9; 10 mM KCl; 1.5 mM MgCl; 1.5% NP-40 and 1 mM PMSF) and centrifuged at 10,000 *g* for 5 minutes at 4°C to generate supernatants containing the cytosolic and membrane proteins. The pellets were used for nuclear extraction using a high-salt lysis buffer (20 mM HEPES-KOH pH 7.9; 1.22 mM MgCl; 420 mM NaCl; 0.2 mM EDTA; 25% glycerol; 1 mM NaF; 1 mM Na_2VO_3; 0.5 mM DTT; and 1 mM PMSF), and spun at 10,000 *g* for 5 minutes at 4°C to generate supernatants containing nuclear extracts. Protein concentration was measured using Bio-Rad protein assay kit. Proteins were separated by SDS-PAGE and transferred onto nitrocellulose membranes (Invitrogen, Carlsbad, CA). Western blots were processed at room temperature as described (Lecanda et al., 2000) using either the PEP.1 antibody (1:500) or N-cadherin (N19) antibody (1:1000; Santa Cruz), or an anti-β-catenin antibody (1:5000; Upstate, Charlottesville, VA), and visualized by ECL detection. In some cases, the membranes were washed an re-probed with an anti-GAPDH antibody to control for loading.

Retroviral transduction of active β-catenin

Retroviral particles were generated as described previously (Lai et al., 2001) by transfecting the SFG viral vector containing the mutant β-catenin construct ΔN151 into the packaging cells 293GPG, which express MuLV gag-pol and vesicular stomatitis virus G glycoprotein under tetracycline regulation, using LipofectAMINE (Gibco, Grand Island, NY). To clone ΔN151 into SFG, the pUHD10-3/ΔN151 vector (kind gift of Dr James Nelson, University of California San Francisco) was digested with *Nco*I, blunt-ended, and then released with *Bam*HI. The insert was then blunt-end ligated into the *Bam*HI site of SFG. In order to generate the highest titer of viral particles (>5×10^6 CFU/ml), conditioned medium was harvested daily from day 3 to day 7 after the withdrawal of tetracycline. The media were combined, filtered through a 0.45 µm membrane and used for transduction in the presence of 8 µg/ml polybrene. As a negative control, a virus carrying the SFG-LacZ cDNA was generated in the same fashion. Retroviral transduction was performed either the day after seeding (CLVC), or after 5 days in culture (BMSC), by adding conditioned medium containing either ΔN151 or LacZ retroviral particles, and incubating for 24 hours. These conditioned media were not cytotoxic based on pilot titration experiments. At the end of the incubation period, the virus-containing medium was removed,

Fig. 1. Development of NcadΔC transgenic mice. (A) Linearized structure of the OG2-NcadΔC construct used for transgenic expression. The 1.1 kb *Pst*I fragment was used as a probe in Southern analysis, and the two arrows identify the primers used for PCR genotyping. Both the cDNA probe and the ~250 kb PCR product encompass the junction between the OG2 promoter and the 5′ end of the NcadΔC reading frame, thus making them specific for the transgene. (B) Southern blot (upper panel) and PCR (lower panel) of genomic DNA of one mouse litter showing a 1.1 kb band or a ~250 bp product, respectively, corresponding to the transgene. (C) Detection of transgene expression by reverse transcription and PCR of total RNA extracted from tissues of 2-month-old transgenic animals, showing a ~195 bp band corresponding to NcadΔC mRNA only in extracts from calvaria and femurs, but not from other tissues. Control reactions were run either in the absence of reverse transcriptase (No RT) or in the presence of NcadΔC plasmid, as indicated. Amplification of GAPDH was used to control for mRNA integrity and PCR efficiency. (D) Total protein extracts of mouse calvaria isolated from either OG2-NcadΔC (Tg) or wild-type (WT) animals were immunoprecipitated (IP) using the PEP.1 antibody that recognizes the intracellular tail of *Xenopus* N-cadherin. Proteins in the whole-cell lysate (input) and in the immunoprecipitate (beads) were separated by SDS-PAGE and blotted (WB) using an anti-FLAG antibody. A band of ~45 kDa, corresponding to the truncated NcadΔC, was detected in the immunoprecipitate from transgenic animals, but not from wild-type littermates. The higher molecular weight bands represent IgG heavy chain.
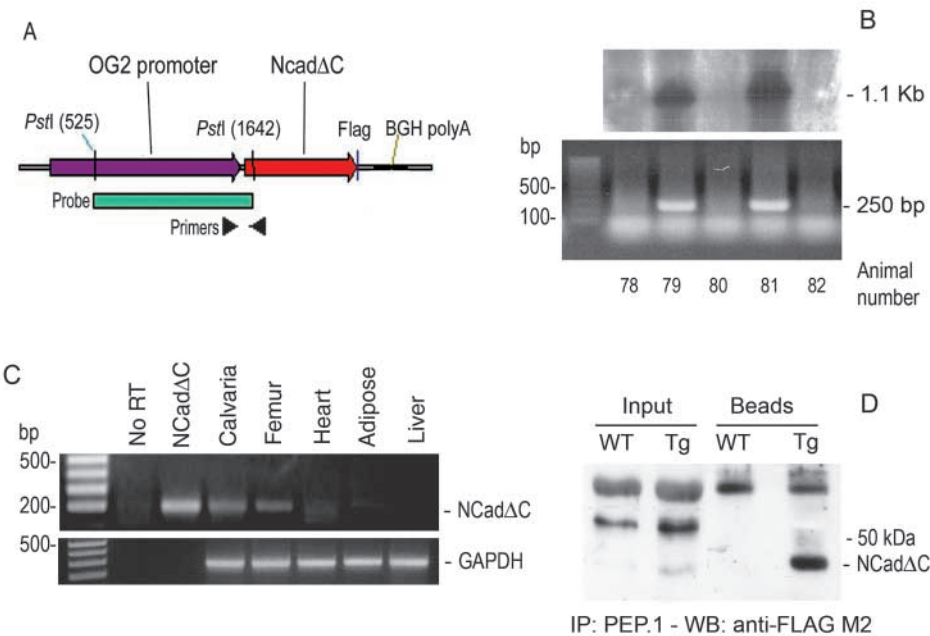

Table 1. List of primers used in this work

Primer sets used for RT-PCR

Gene product	Forward primer	Reverse primer	Product size (bp)
NcadΔC	AAACAGCCCTTCCTGCTACC	TCATGCTCAGAAGAGGAGACC	195
GAPDH	ACTTTGTGAAGCTCATTTCC	TGCAGCGAACTTTATTGATG	265

Primer sets used in real-time RT-PCR

Gene product	Forward primer	Reverse primer
PPARγ2	ACCACTCGCATTCCTTTGAC	TGGGTCAGCTCTTGTGAATG
Adipsin	TGCATCAACTCAGAGGTGTCAATCA	TGCGCAGATTGCAGGTTGT
Cbfa1	CCGTGGCCTTCAAGGTTGT	TTCATAACAGCGGAGGCATTT
Colα1(I)	GATGACGTGCAATGCAATGAA	TGATAGTATTCTTCCGGGCAGAAA
Osteopontin	GTATTGCTTTTGCCTGTTTGG	TGAGCTGCCAGAATCAGTCAC
Osteoprotegerin	TCCCGAGGACCACAATGAAC	TGGGTTGTCCATTCAATGATGT
RANK-L	CCTGAGGCCCAGCCATTT	GGTACCAAGAGGACAGAGTGACTTTA

and cells were grown according to the procedures described for the CFU assays.
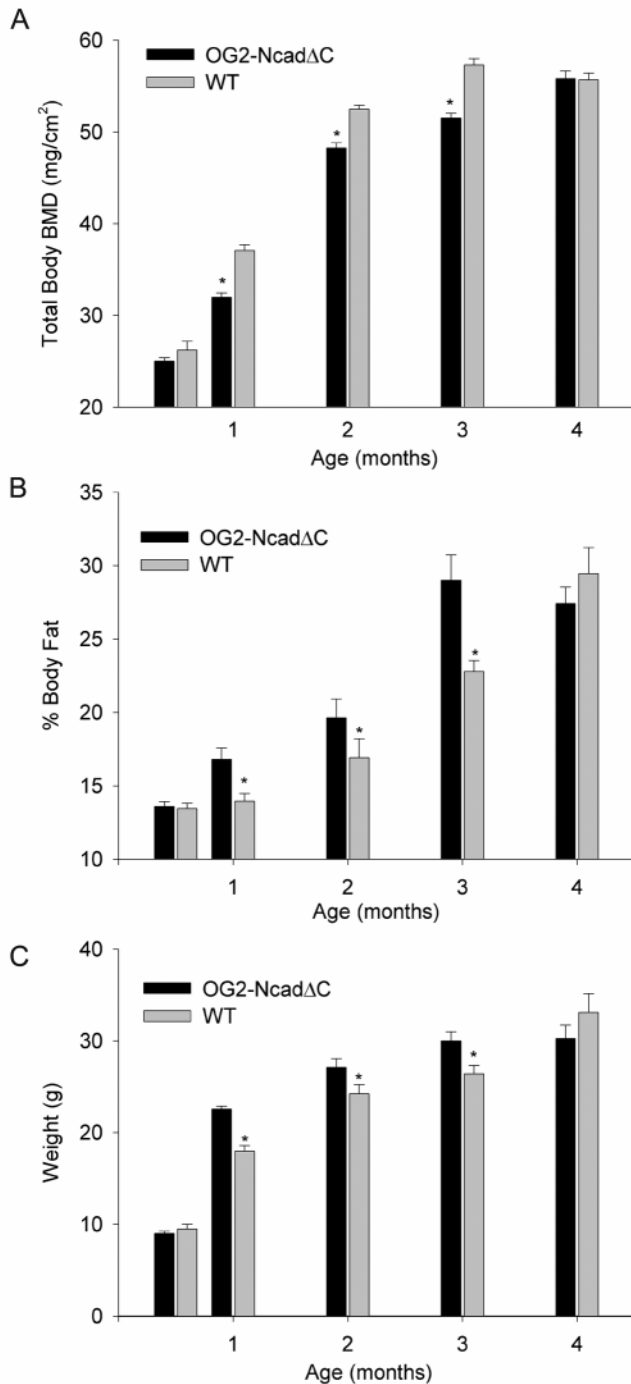
Reverse transcription and PCR (RT-PCR)

Femurs were dissected out, cleaned of soft tissue and snap frozen in liquid nitrogen then homogenized using a mortar and pestle. Total RNA was extracted using TRIzol (Gibco) according to manufacturer's directions. BMSC and CLVC were cultured in αMEM medium containing 10% FCS for 3-4 weeks and total RNA isolated as just described. For RT-PCR, 1 μg of total RNA was reverse transcribed using oligo-dT primers and Moloney Murine Leukemia Virus reverse transcriptase (Invitrogen) in a 20 μl reaction. Reverse transcription was carried out for 60 minutes at 42°C. The temperature was then raised to 95°C for 15 minutes to inactivate the transcriptase and

activate the polymerase, and first strand cDNA was amplified by 35 cycles (94°C for 1 minute, 55°C for 1 minute, 72°C for 1 minute, and 72°C for 10 minutes). The presence of NcadΔC mRNA was detected using primers that amplify a fragment of the NcadΔC coding region (bases 52 to 246), yielding a 195 bp product. GAPDH was used as an internal control for cDNA quality and PCR efficiency (Table 1). The reaction products were separated on a 2% agarose gel electrophoresis, and visualized by ethidium bromide staining.

Real time-RT-PCR

Total RNA (1 μg) isolated from CLVC and BMSC was reverse transcribed using Superscript II reverse transcriptase and oligo(dT)15 primers. One fiftieth of this reaction was used for real-time PCR analysis of mRNA using the SYBR green PCR method according to

Fig. 2. Low bone mass and high body fat in OG2-NcadΔC mice. Bone density and body composition were analyzed by dual energy X-ray absorptiometry in live animals at different times up to 4 months. (A) Total body bone mineral density (BMD) was significantly reduced in OG2-NcadΔC mice during the first 3 months of age – when BMD accumulates – compared with wild-type littermates, whereas percent body fat (B) and body weight (C) were significantly higher in OG2-NcadΔC mice compared with wild-type littermates during the first 3 months of age. *$P<0.05$, two-way ANOVA. Error bars represent standard deviation.
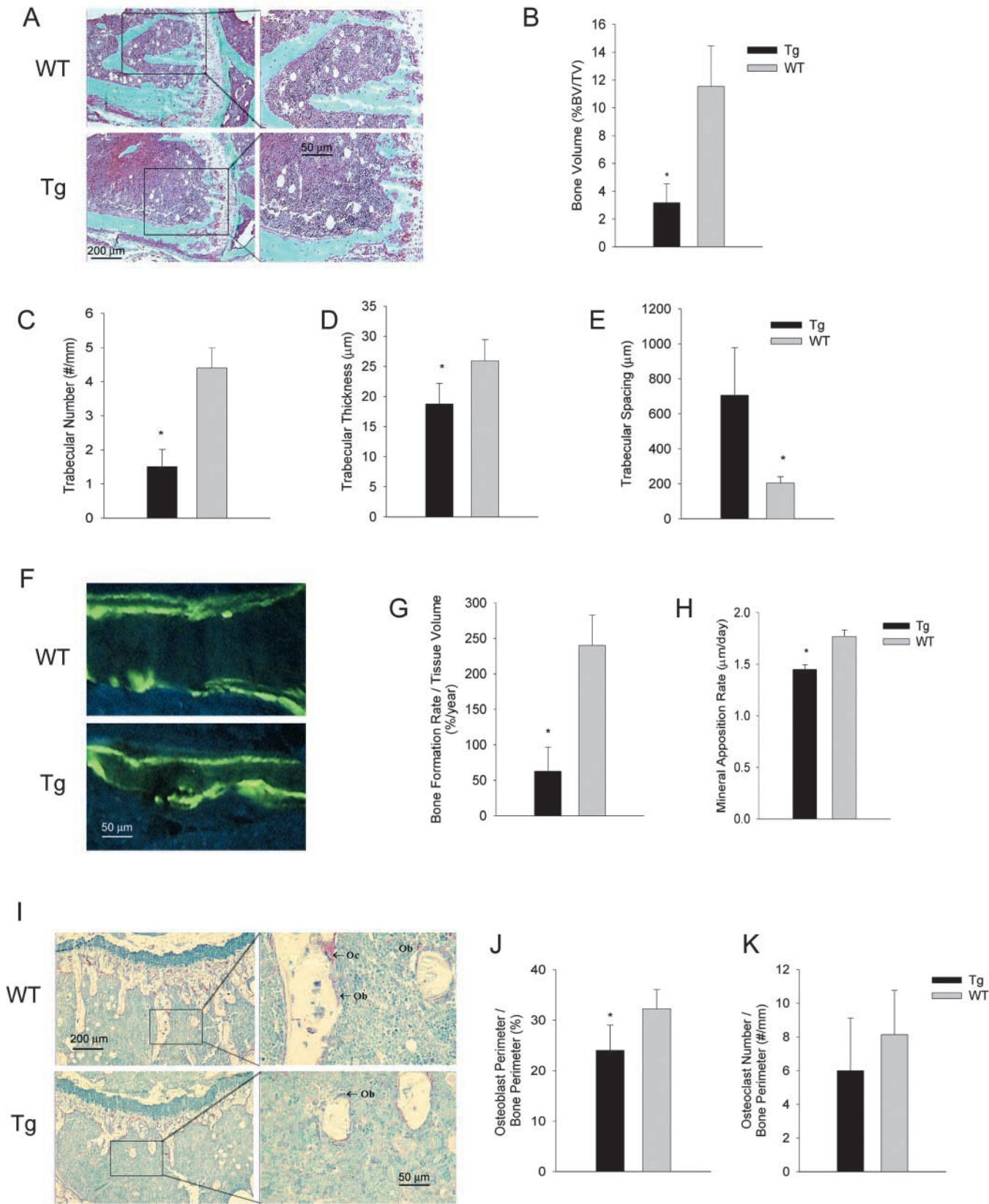
Results

Selective expression of the NcadΔC transgene in cells of the osteoblastic lineage

We used the OG2 promoter (1.3 kb) to express the truncated cadherin mutant NcadΔC selectively in osteoblasts, because it had previously been shown to drive the in vivo expression of other genes in bone forming cells only postnatally (Ducy et al., 1999). To establish an OG2-NcadΔC homozygous transgenic line, we identified five founder transgenic mice among 25 pups produced after reimplantation of the microinjected embryos. We selected two founder male mice for high copy number of the transgene, and mated them with wild-type B3CF1 female mice. Hemizygous F1 transgenic animals were then cross-bred to produce homozygous F2 animals. The presence of NcadΔC transgene transcript was confirmed as a 195 bp band detected by RT-PCR in extracts of femur and calvaria of OG2-NcadΔC mice, but not in extracts from other tissues (Fig. 1C), thus confirming osteoblast-specific expression of the transgene. Expression of NcadΔC protein in bone was detected by immunoprecipitation using an antibody that recognizes the intracellular tail of *Xenopus* N-cadherin (PEP.1) and subsequent western analysis using an anti-FLAG M2 antibody that recognizes the epitope tag fused to the NcadΔC construct. A band of approximately 45 kDa, corresponding to the truncated NcadΔC, was detected in the input fraction from transgenic calvarium and was markedly enriched in the immunoprecipitated fraction (Fig. 1D, lanes 2 and 4). The 45kDa protein was not detected in protein extracts from wild-type littermate calvarium (Fig. 1D, lanes 1 and 3).

Low bone mass and high body fat phenotype in OG2-NcadΔC mice

As shown in Fig. 2A, during the first 3 months of life – when bone mass accumulates – total body bone mineral density was consistently reduced in transgenic animals compared with wild-type littermates, with maximal difference of 10% at age of 3 months (51.54±2.01 mg/cm^2, $n=26$; vs. 57.3±2.45 mg/cm^2, $n=13$; $P<0.001$; respectively). Thereafter, no statistically significant difference in bone density was detected between wild-type and transgenic mice. By contrast, body composition analysis showed reciprocal changes at the earliest time-points, with consistently higher percent body fat in OG2-NcadΔC relative to wild-type mice (Fig. 2B), and maximal difference of 27% at 3 months of age (29±5.7% vs. 22.8±2.3%; $P=0.011$). During the same time period, body weight (Fig. 2C) and food intake were also significantly higher in OG2-NcadΔC mice than in wild-type controls (4.59±0.67 g/day vs. 3.03±0.33 g/day; $P<0.01$). At age 4 months and higher, percent body fat and body weights were no longer different between mutant and wild-type animals.

manufacturer's instruction (PE Biosystems, Foster City, CA). In brief, a mixture of 1× SYBR green master mix, 50 nM forward primer and 50 nM reverse primer with the cDNA template (2 μl) was heated at 95°C for 10 minutes. DNA was then amplified for 40 cycles (95°C for 15 seconds, 60°C for 1 minute) on the GeneAmp 5700 sequence detector. The primers used are listed in Table 1. GAPDH (PE Biosystems) was used as internal control. The cycle number at which the fluorescence exceeded the threshold of detection (CT) for GAPDH was subtracted from that of the target gene product for each well (ΔCT). Transcription level of expression, relative to wild-type controls, was defined as ($2^{-\Delta\Delta CT}$), where ΔΔCT equals the OG2-NcadΔC ΔCT minus the ΔCT of wild-type cells. All real-time PCR experiments were performed at least three times.

Histomorphometric analysis of long bones revealed an even more pronounced low bone mass phenotype in OG2-NcadΔC transgenic mice than was detected by radio-absorptiometric measurements. Trabecular bone volume in the proximal tibial metaphysis was reduced 73% in 2-month-old transgenic mice relative to wild-type littermates (Fig. 3A,B). This decreased bone volume was associated with a decrease in trabecular number and thickness, and a significant increase in the mean

Fig. 3. Reduced bone formation in OG2-NcadΔC transgenic mice: histologic and histomorphometric analysis. (A) Goldner's trichrome stained, 4 μm undecalcified sections of proximal tibiae from OG2-NcadΔC (Tg) or wild-type (WT). Micrographs on the right are enlargements (400×) of the rectangular areas shown on the left micrographs (200×). (B) Bone volume, expressed as a percentage of total tissue volume (BV/TV) in the entire area of the bone marrow cavity 175-875 μm from the growth plates was significantly reduced in transgenic mice compared with those of wild-type controls (*n*=8). (C-E) OG2-NcadΔC mice also exhibited a significantly lower trabecular number and thickness and higher trabecular separation compared with wild-type mice. (F) Fluorescence micrograph of calcein labeling in 8 μm unstained sections of cancellous bone, showing no double labels in sections of transgenic mice bone. Accordingly (G,H), dynamic parameters of bone formation, bone formation rate/tissue volume and mineral apposition rate were significantly reduced in transgenic mice compared with wild-type littermates. (I) Four-micrometer sections of proximal tibiae were stained for tartrate resistant acid phosphatase activity and counterstained with methyl green and thionin for identification of osteoclasts (Oc) and osteoblasts (Ob). Micrographs on the right are enlargements (400×) of the rectangular areas shown on the left micrographs (200×). (J,K) The number of osteoblasts expressed as osteoblast perimeter per bone perimeter (%) was reduced in OG2-NcadΔC mice compared with wild-type mice. There was no significant difference in the number of osteoclasts between transgenic and wild-type animals. In all panels, asterisks denote *P*<0.05, *t*-test.

distance between individual trabeculae (Fig. 3C-E). Dynamic indices of bone formation suggested an osteoblast defect in transgenic animals, reflected by a few double labeled seams and reduced distance between the two calcein labels visualized by fluorescence microscopy (Fig. 3F). Bone formation rate was reduced 74% in OG2-NcadΔC mice (Fig. 3G), commensurate with the decreased bone volume, and mineral apposition rate was also significantly reduced (Fig. 3H). The number of osteoblasts was lower in transgenic than in wild-type mice (Fig. 3I,J), although the difference was not as large as that seen for bone formation rate. However, there was no significant difference in osteoclast number between transgenic and wild-type animals in sections stained for the osteoclast-specific tartrate-resistant acid phosphatase activity (Fig. 3K). There were also no differences in osteoid labeling or thickness, or in the width of the growth plate between wild-type and transgenic mice (89.57±1.46 vs. 81.40±6.69 μm, respectively).

NcadΔC expression in vivo retards osteoblast differentiation
We next examined osteoblast differentiation and function in cells isolated from newborn mouse calvaria. As shown in Fig. 4A, alkaline phosphatase activity, an index of osteogenic differentiation, was reduced after 1 and 2 weeks post-confluence in CLVC derived from OG2-NcadΔC mice compared with wild-type controls, but it was not different after 3 weeks in culture. Matrix mineralization was modestly but not substantially reduced in mutant relative to wild-type cells cultured for 2 and 3 weeks after confluence in the presence of AA and β-GP, despite expression of the transgene at these time-points (Fig. 4B). However, using the highly sensitive real time RT-PCR we did find that expression of many osteoblast products was indeed

altered in OG2-NcadΔC CLVC after 2 weeks of culture. The abundance of mRNA transcripts for Cbfa1, osteopontin, osteoprotegerin and RANK-L were all reduced in OG2-NcadΔC relative to wild-type cells, whereas type I collagen expression was slightly higher 2 weeks post-confluence (Fig. 4B). Detection of osteocalcin mRNA yielded inconsistent results, but because we used the OG2 promoter to drive expression of NcadΔC, which in turn alters osteoblast differentiation, the interpretation of osteocalcin expression data is problematic. Using the PEP.1 antibody in immunoblots or an antibody against the N-terminus of mouse N-cadherin (N19) in immunoprecipitations, we did not detect any differences in endogenous N-cadherin abundance between transgenic and wild-type cells (Fig. 4D), consistent with our previous findings in osteoblastic cells showing that NcadΔC expression alters the function but not the expression of osteoblast cadherins (Cheng et al., 2000).

## NcadΔC expression in vivo alters bone marrow mesenchymal cell differentiation
To test whether the ability to generate osteogenic precursors was defective in OG2-NcadΔC mice, we analyzed lineage allocation by bone marrow mesenchymal precursors using a limiting dilution method. As shown in Fig. 5A, unfractionated BMSC from OG2-NcadΔC mice seeded at low density and then cultured in mineralizing medium for 3 weeks yielded a significantly lower number of Von Kossa positive wells relative to wild-type cultures, resulting in 50% fewer CFU-O than wild-type controls (Fig. 5C). Conversely, OG2-NcadΔC BMSC cultures incubated with an adipogenic cocktail (IBMX, indomethacin and hydrocortisone) generated a higher number of cells positive for Oil Red O lipid droplets relative to wild-type cultures (Fig. 5B), resulting in fivefold higher CFU-A relative to wild-type controls (Fig. 5C). But the number of CFU-F, an index of mesenchymal cell precursor number, did not differ between the two genotypes (Fig. 5C).

The evidence of an osteoblastogenic to adipogenic shift was corroborated by quantitative real-time PCR assessment of molecular markers of mesenchymal cell differentiation. The abundance of mRNA for PPARγ2, one of the earliest transcription factors that are expressed in the adipogenic pathway, and for adipsin, a marker of terminally differentiated adipocytes, were 11-fold and 3-fold higher, respectively, in OG2-NcadΔC BMSC cultures than in wild-type cells (Fig. 5D). By contrast, the abundance of Cbfa1 mRNA, one of the earliest transcriptional factors expressed during the osteoblast differentiation program, was decreased 40% in OG2-NcadΔC marrow cells compared to wild-type cultures. Confirming expression of the transgene in these conditions, a PCR product of the correct size was amplified from cDNA obtained from cultures of BMSC isolated from transgenic mice only after culture in mineralizing medium to allow for osteoblast differentiation (Fig. 5E). The PCR product was not present in freshly isolated, undifferentiated BMSC (not shown).

Viral transduction of constitutively active β-catenin rescues the osteoblast defect and reduced adipogenic commitment in NcadΔC cells
Expression of the truncated NcadΔC mutant can theoretically not only interfere with cell-cell adhesion, as we previously

Fig. 4. NcadΔC expression in vivo retards osteoblast differentiation. (A) Calvaria cells (CLVC) were cultured in 24-well plates up to 3 weeks after confluence, and alkaline phosphatase activity was measured in the cell layer at weekly intervals, and normalized to cellular protein content. Enzyme activity was reduced in CLVC from newborn OG2-NcadΔC mice compared with wild-type (WT) cells at 1 and 2 weeks post-confluence. *$P<0.001$, t-test (mean±s.e.m.). (B) Von Kossa staining of CLVC cultures isolated from newborn OG2-NcadΔC transgenic (Tg) or wild-type (WT) mice, after 2 or 3 weeks in culture in the presence of AA (50 μg/ml) and β-GP (10 mM). There is no apparent difference in the mineralized (dark stain) area between the transgenic and wild-type cells at either time-point. Expression of the transgene NcadΔC was detected at the corresponding time-points by RT-PCR of total RNA extracted from parallel cultures, with GAPDH as control for RNA integrity and abundance (lower panels). (C) Total RNA was extracted from CLVC grown for 2 weeks after confluence. The amount of mRNA for osteoblast products was determined by real-time PCR and expressed as mRNA abundance in OG2-NcadΔC relative to wild-type (WT) cells. Type I collagen expression levels were increased 1.8 times in transgenic animals compared with wild-type controls, whereas osteoprotegerin, osteopontin, Cbfa1 and RANK-L mRNA abundance was significantly reduced. (D) Whole-cell lysates obtained from transgenic (Tg) and wild-type (WT) CLVC grown for 3 weeks post-confluence were separated by SDS-PAGE and blotted using antibodies that recognize the intracellular tail of *Xenopus* N-cadherin (PEP.1) or the N-terminus of N-cadherin (N19; Santa Cruz). Two bands of ~100 and 120 kDa were detected in both cases, corresponding to endogenous N-cadherin and possibly other cross-reacting cadherins. A band of ~45 kDa, corresponding to the truncated NcadΔC, was detected by the PEP.1 antibody only in CLVC from transgenic animals, but not from wild-type littermates (left panel). This membrane was stripped and blotted again with an anti-GAPDH antibody to control for loading.
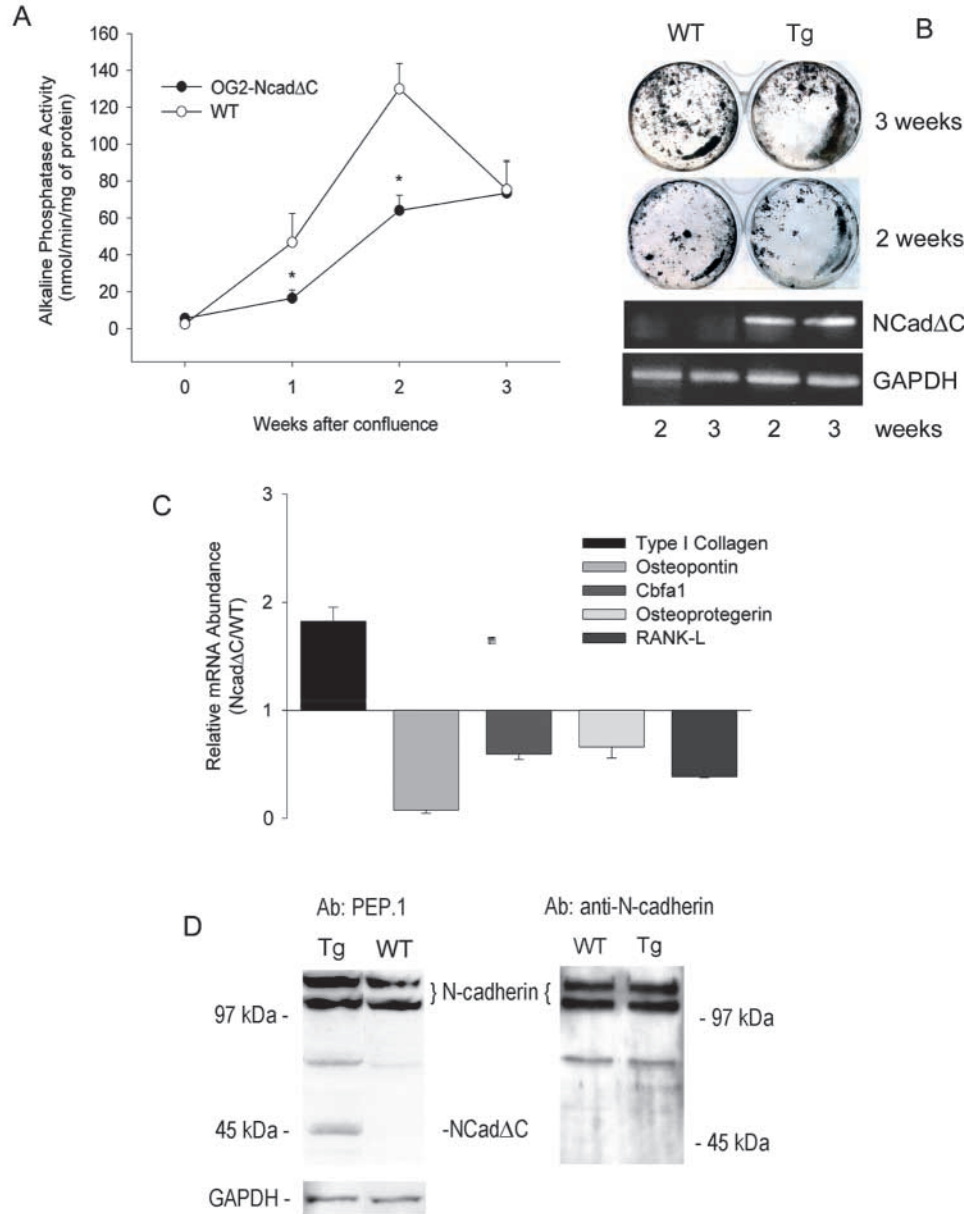
showed (Cheng et al., 2000), but it can also sequester β-catenin in the plasma membrane, reducing its cytoplasmic pool and thus inhibiting its transcriptional activity (Fujimori and Takeichi, 1993). To explore this possibility, we first determined the cellular distribution of β-catenin in NcadΔC-expressing cells. Cell fractionation of β-catenin showed that in calvaria cells isolated from newborn mice, the abundance of nuclear β-catenin was lower in transgenic than in wild-type cells, whereas the cytosol/membrane fraction was slightly higher (Fig. 6A, left). Such differences in β-catenin cellular distribution were not observed in BMSC isolated from long bones of 4-month-old mice (Fig. 6A, right). We then introduced a mutated form of β-catenin, ΔN151, into CLVC using a retroviral vector. This

mutant construct lacks the ubiquitination domain, does not undergo proteasome degradation and remains transcriptionally active (Zhu and Watt, 1999). As shown in Fig. 6B, ΔN151 transduction in OG2-NcadΔC CLVC significantly increased alkaline phosphatase activity compared with nontransduced OG2-NcadΔC cells, restoring the enzyme activity to that seen in wild-type cells. The active β-catenin mutant had no effect on alkaline phosphatase activity in wild-type cells. A reciprocal effect was obtained by transduction of ΔN151 into BMSC cultures from OG2-NcadΔC mice; active β-catenin inhibited the exuberant adipogenic differentiation of OG2-NcadΔC BMSC, restoring the number of CFU-A to normal, without effects in wild-type cells (Fig. 6C).

Fig. 5. Reduced osteoblastogenesis and increased adipogenesis of OG2-NcadΔC bone marrow cells. (A) Bone marrow stromal cells (BMSC) isolated from 2-month-old mice were cultured in 96-well plates in the presence of AA (50 µg/ml) and β-GP (10 mM) for 4 weeks at low density (3.2×10^3 cell/cm^2) for limiting dilution analysis of CFU-Osteoblast, determined by Von Kossa staining. Relative to wild-type cells (WT), there was a lower number of von Kassa-positive wells in BMSC cultures isolated from OG2-NcadΔC (Tg) mice. (B) BMSC from OG2-NcadΔC and wild-type mice were cultured in the presence of an adipogenic cocktail (0.5 mM IBMX, 60 µM indomethacin, and 0.5 µM hydrocortisone) for 2 weeks and the number of CFU-Adipocyte was determined by Oil red O staining. A higher abundance of lipid droplet-positive cells was detectable even in cultures seeded at high density in cells from transgenic mice (10^5 cells/cm^2). Representative photomicrographs of wild-type and OG2-NcadΔC BMSC cultures stained with Oil Red O are shown on the right. (C) The number of CFU-Osteoblast was significantly lower, and the number of CFU-Adipocyte was significantly higher in transgenic compared with wild-type BMSC cultures, assessed by limiting dilution analysis ($n=5$); *$P<0.05$, t-test. (D) The abundance of PPAR-γ2, adipsin and Cbfa1 mRNA was assessed by real-time RT-PCR in BMSC cultures after 2 weeks of culture in the absence of stimulators. There was a significant increase in PPAR-γ2 and adipsin mRNA abundance in cells derived from OG2-NcadΔC animals compared with wild-type littermates, whereas Cbfa1 mRNA was reduced 40%. (E) Expression of the transgene, NcadΔC was detected after 2 weeks of culture by RT-PCR of total RNA extracted from parallel cultures, with GAPDH as control for RNA integrity and abundance (lower panels). No PCR products were obtained in the absence of reverse transcriptase (RT), thus excluding DNA contamination.
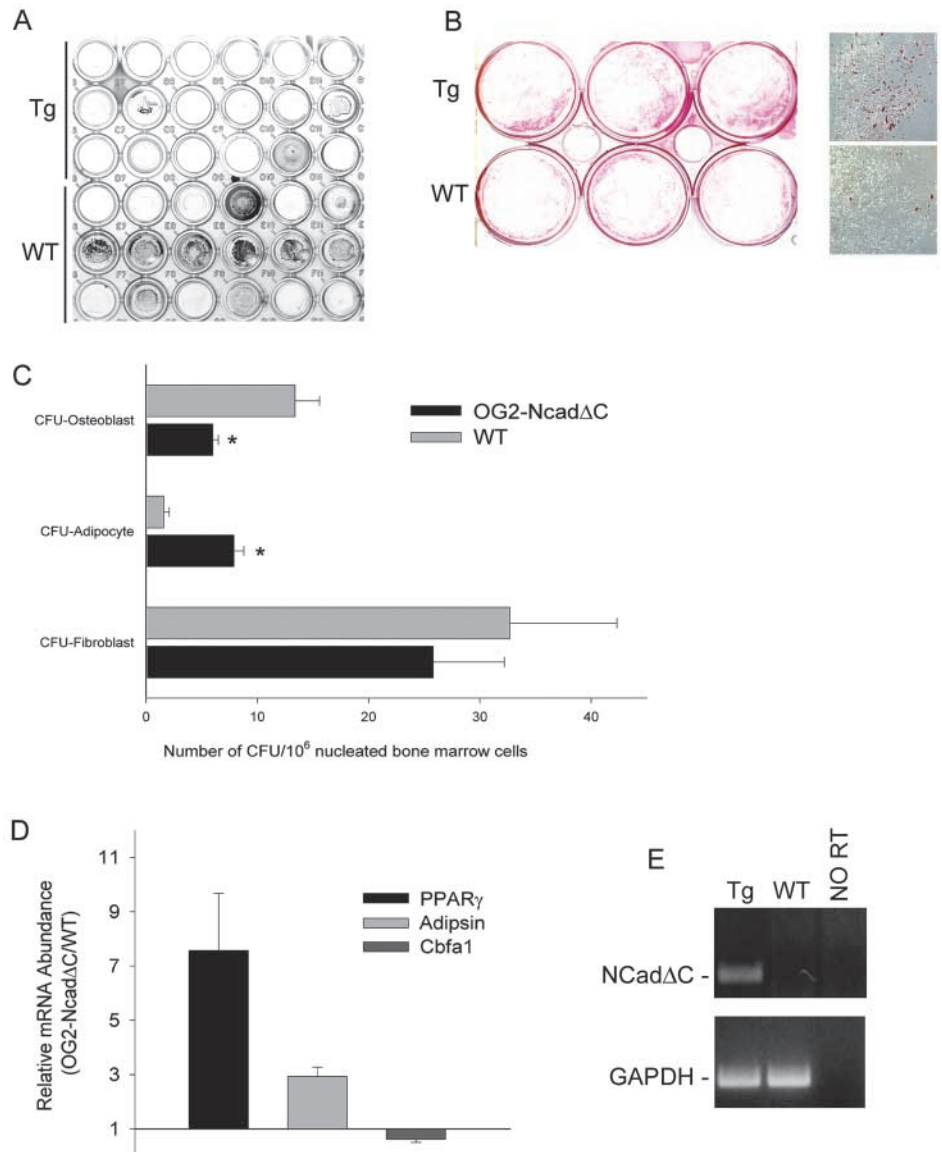
Discussion

We have shown that in vivo expression of a dominant-negative cadherin, NcadΔC, in osteoblasts leads to transient osteopenia and increased adiposity in mice. Expression of this truncated cadherin in osteoblasts in vivo interferes with the osteoblast differentiation program and shifts bone marrow mesenchymal cell commitment from osteogenesis to adipogenesis. In vitro, the osteoblast abnormality can be reversed by expression of a stabilized, active β-catenin mutant. Thus, the integrity of cadherin function in osteoblasts is necessary for the differentiation and function of bone forming cells.

The osteopenia of young transgenic animals was global, as determined by whole body bone mineral density, but it was particularly evident on the trabecular component of long bones, where the decrease of trabecular bone volume was >50% at 2 months. Histologically, the osteopenic phenotype of young NcadΔC transgenic mice is the consequence of decreased bone formation rate and perhaps reduced osteoblast number, but not increased bone resorption. The inherent high variability in the histomorphometric measurements of osteoblast number and the less distinctive morphologic features of mouse osteoblasts compared with rat or human osteoblasts (Jilka et al., 1996) may explain the only modestly reduced osteoblast number compared with the dramatically decreased dynamic indices of bone formation in transgenic mice. Very consistent with our findings is a similar, though milder, osteopenic phenotype observed in 3-month-old mice genetically deficient in cadherin-11 (Kawaguchi et al., 2001a). Although the authors did not report whether the low bone mass corrected with time in older animals, they did observe decreased bone formation rates in cadherin-11 deficient mice. The relatively more severe osteopenia in our mice, a model of global, non-isotype specific interference with cadherin function may indicate that other cadherins are involved in control of bone formation. The most

Fig. 6. Altered β-catenin subcellular distribution and effect of viral transduction of constitutively active β-catenin in OG2-NcadΔC cells. (A) The cytosolic/membrane and nuclear fractions of calvaria cells (CLVC) isolated from newborn OG2-NcadΔC (Tg) or wild-type (WT) mice (left panel) or of bone marrow stromal cells (BMSC) isolated from 4-month-old mice (right panel) were separated as described in Materials and Methods, and blotted using an antibody that recognizes the cytoplasmic tail of N-cadherin. Note that OG2-NcadΔC-expressing cells exhibited more abundant β-catenin in cytosol/membrane compartments and lower β-catenin abundance in the nuclear fraction, relative to wild-type cells. The distribution of β-catenin between cytosol/membrane and nuclear compartments is similar in transgenic and wild-type cells. (B) OG2-NcadΔC and wild-type CLVC were transduced with retroviral vectors expressing either the stable, constitutively active β-catenin construct, ΔN151 or LacZ, and cultured for 2 weeks before determination of alkaline phosphatase activity. Transduction of β-catenin increased enzyme activity in OG2-NcadΔC CLVC to levels similar to those present in wild-type cells, whereas no effect was seen in either nontransduced cells or cells exposed to LacZ retrovirus. (C) OG2-NcadΔC and wild-type BMSC were transduced with the ΔN151 or LacZ retroviral vectors, as just described, and grown for 2 weeks for CFU-Adipocyte determination. Transduction of β-catenin reduced the number of CFU-Adipocyte in OG2-NcadΔC BMSC to levels similar to those present in wild type cells, while transduction of LacZ was ineffective; *$P<0.05$, *t*-test (mean±s.e.m.). All data are representative or the average of at least three different experiments.
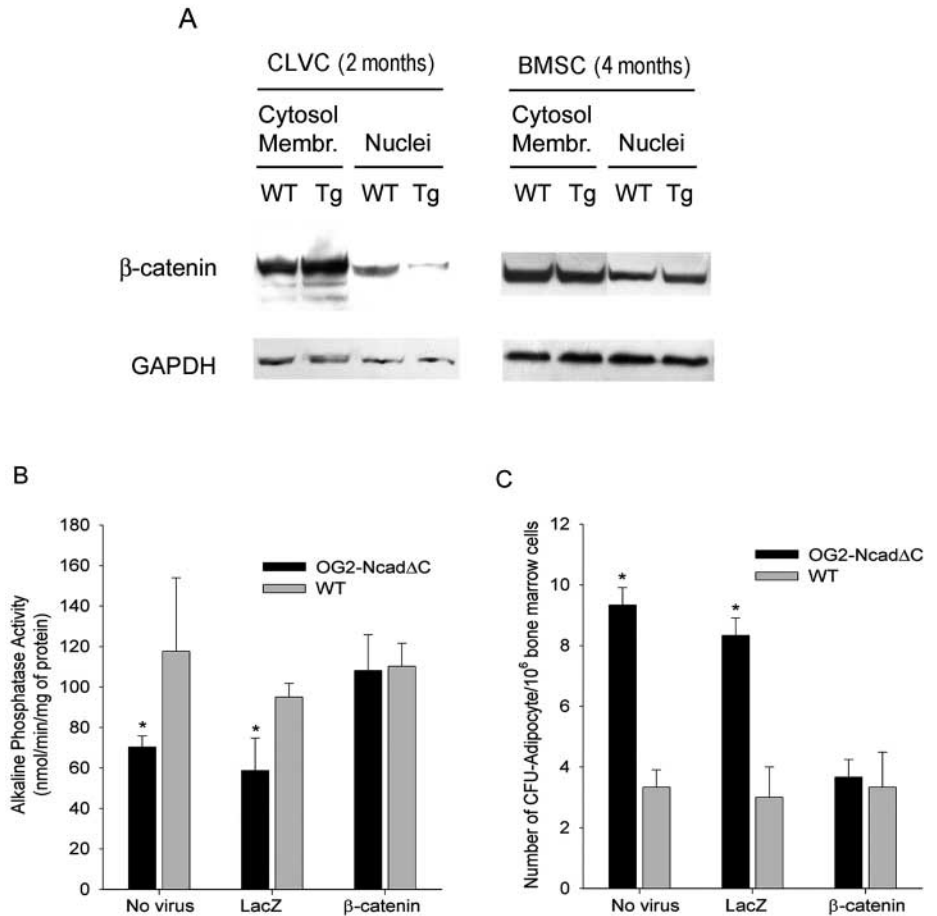
likely candidate is N-cadherin, which is abundantly expressed in osteogenic cells and known to be involved in chondro-osteogenesis (Haas and Tuan, 1999; Marie, 2002; Tuan, 2003). As NcadΔC did not affect expression of endogenous osteoblast cadherins, a finding consistent with our previous results in MC3T3-E1 cells (Cheng et al., 2000), it is likely that the phenotype we observed is related to an interference of the dominant-negative transgene with cadherin-regulated signaling, as discussed further below. The mechanism by which peripheral fat is increased in OG2-NcadΔC mice is under investigation, but it may be related to the exuberant adipogenesis induced by the dominant-negative cadherin (see below). It is interesting to note that the reciprocal changes in body fat and bone mass simultaneously correct at 4 months of age, pointing to a common cause. We were able to detect the presence of NcadΔC mRNA in osteoblasts up to 6 months of age (data not shown), thus ruling out inactivation of the OG2 promoter as an explanation for the transient phenotype. Although the reasons for the recovery of bone mass at 4 months remain unexplained, normalization of β-catenin cellular distribution in BMSC suggests that cadherin-independent compensatory mechanisms might reverse the abnormality of β-catenin signaling induced by the dominant-negative cadherin by 4 months of age.

At the cellular level, the reduced development of alkaline phosphatase activity and the lower abundance of most osteoblast-specific products, osteopontin, osteoprotegerin, RANK-L and, in particular, Cbfa1, in post-confluent CLVC cultures (which consist of fully committed osteogenic cells), suggest a disruption of the osteoblast differentiation program by NcadΔC. The modest increase of type I collagen mRNA in NcadΔC in CLVC, a finding also previously noted in the MC3T3-E1 cell line (Cheng et al., 2000), may simply reflect a slow progression to full differentiation in the genetically altered cell cultures, as production of type I collagen decreases with full differentiation. However, in vitro CLVC mineralization was only modestly affected by NcadΔC expression. It should be noted that CLVC cultures are tested when fully confluent, and in such conditions the number of osteoblasts that are able to fully differentiate may be sufficient to produce substantial mineralized matrix, thus masking subtle differences. However, the osteogenic to adipogenic shift in bone marrow precursor cell differentiation was unexpected, since the transgene is driven by the mouse OG2 promoter, which is expressed in mature, differentiated osteoblasts (Ducy et al., 1999), and thus should not be present in undifferentiated cells. In fact, we could detect the transgene in BMSC only when these cells were pushed towards osteoblast differentiation by incubation with AA and β-GP. Yet, the reciprocal down- and upregulation of early, lineage-specific

transcription factors, Cbfa1 and PPARγ2, implies an alteration of early commitment. Perhaps the lower number of cells that can go through the osteogenic pathway in the presence of the dominant-negative cadherin may simply increase the number of uncommitted cells that will default to the adipogenic pathway. Another more intriguing possibility may be that differentiated osteoblasts release signals that feedback onto uncommitted precursors and regulate their fate. Disruption of such signals by dominant-negative cadherin may negatively affect mesenchymal cell commitment towards osteogenesis. Whichever the mechanism, the present in vivo results strengthen previous in vitro work from our and other groups, showing that cadherins are critically involved in chondro-osteogenic differentiation. In uncommitted C3H10T1/2 and C2C12 mesenchymal cells, stimulation of osteoblast differentiation is associated with increased expression of N-cadherin and cadherin-11, whereas the abundance of these two cadherins decreases with adipogenic differentiation, to completely disappear in fully differentiated adipocytes (Shin et al., 2000; Kawaguchi et al., 2001b). Likewise, N-cadherin is critically involved in cell-cell interactions during TGF-β-induced cartilage condensation, and it is sequentially up- and downregulated in chondrogenesis (Tuli et al., 2003).

The increased membrane/cytoplasmic and decreased nuclear localization of β-catenin in CLVC of young transgenic mice is consistent with others' reports indicating that NcadΔC can retain β-catenin on the cell surface (Kintner, 1992; Fujimori and Takeichi, 1993). A decreased nuclear β-catenin pool may reduce β-catenin available for binding to Tcf/Lef, thus inhibiting its transcriptional activity (Orsulic et al., 1999; Sadot et al., 1998; Fagotto et al., 1996). This mechanism of action is not specific for any cadherins and provides a global inhibition of cadherin-mediated cell-cell adhesion – via interference with lateral clustering and dimerization of endogenous cadherins – and β-catenin signaling (Nieman et al., 1999). The reversal of both the osteogenic defect in CLVC and the exuberant adipogenesis in BMSC by retroviral transduction of a stable, constitutively active β-catenin mutant strengthens the contention that the dominant-negative effect of NcadΔC is probably related to an interference with the canonical β-catenin signaling pathway. Importantly, the β-catenin mutant we used, ΔN151, lacks the α-catenin binding site (Barth et al., 1997). Although α-catenin seems to have a role in signaling, rescue from the shift in lineage allocation seems to be independent of α-catenin binding, as ΔN151 was fully effective in our system. An emerging body of evidence indicates that activation of the canonical β-catenin pathway provides key regulatory cues in mesenchymal cell fate decisions, favoring chondro-osteogenic differentiation (Rawadi et al., 2003; Fischer et al., 2002; Bain et al., 2003), while inhibiting adipogenesis (Ross et al., 2000; Bennett et al., 2002). The decreased osteogenic and increased adipogenic precursors in OG2-NcadΔC mice is perfectly consistent with these reports, showing that, in addition to Wnt signaling, cadherins are critically involved in regulating β-catenin activity.

In conclusion, our data show that in vivo expression of a truncated cadherin mutant in osteoblasts interferes with their differentiation and function and increases adipogenesis, resulting in decreased bone formation, delayed acquisition of peak bone mass and increased peripheral adiposity in young mice. This phenotype is probably determined by interference of the dominant-negative cadherin with β-catenin signaling. Therefore, cadherins are integral modulator of osteoblast function in vitro and in vivo.

References

Bain, G., Muller, T., Wang, X. and Papkoff, J. (2003). Activated β-catenin induces osteoblast differentiation of C3H10T1/2 cells and participates in BMP2 mediated signal transduction. *Biochem. Biophys. Res. Commun.* **301**, 84-91.

Barth, A. I., Pollack, A. L., Altschuler, Y., Mostov, K. E. and Nelson, W. J. (1997). NH2-terminal deletion of β-catenin results in stable£colocalization of mutant β-catenin with adenomatous polyposis coli protein and altered MDCK cell adhesion. *J. Cell Biol.* **136**, 693-706.

Bellows, C. G. and Aubin, J. E. (1989). Determination of numbers of osteoprogenitors present in isolated fetal rat calvaria cells in vitro. *Dev. Biol.* **133**, 8-13.

Bennett, C. N., Ross, S. E., Longo, K. A., Bajnok, L., Hemati, N., Johnson, K. W., Harrison, S. D. and MacDougald, O. A. (2002). Regulation of Wnt signaling during adipogenesis. *J. Biol. Chem.* **277**, 30998-31004.

Cadigan, K. M. and Nusse, R. (1997). Wnt signaling: a common theme in animal development. *Genes Dev.* **11**, 3286-3305.

Cheng, S. L., Lecanda, F., Davidson, M., Warlow, P. M., Zhang, S. F., Zhang, L., Suzuki, S., St John, T. and Civitelli, R. (1998). Human osteoblasts express a repertoire of cadherins, which are critical for BMP-2-induced osteogenic differentiation. *J. Bone Miner. Res.* **13**, 633-644.

Cheng, S.-L., Shin, C. S., Towler, D. A. and Civitelli, R. (2000). A dominant-negative cadherin inhibits osteoblast differentiation. *J. Bone Miner. Res.* **15**, 2362-2370.

Civitelli, R., Lecanda, F., Jørgensen, N. R. and Steinberg, T. H. (2002) Intercellular junctions and cell-cell communication in bone. In *Principles of Bone Biology* (ed. J. P. Bilezikian, A. R. Rodan and L. G. Raisz), pp. 287-302. San Diego, CA: Academic Press.

Ducy, P. and Karsenty, G. (1995). Two distinct osteoblast-specific *cis*-acting elements control expression of a mouse osteocalcin gene. *Mol. Cell. Biol.* **15**, 1858-1869.

Ducy, P., Starbuck, M., Priemel, M., Shen, J., Pinero, G., Geoffroy, V., Amling, M. and Karsenty, G. (1999). A Cbfa1-dependent genetic pathway controls bone formation beyond embryonic development. *Genes Dev.* **13**, 1025-1036.

Fagotto, F., Funayama, N., Gluck, U. and Gumbiner, B. M. (1996). Binding to cadherins antagonizes the signaling activity of beta-catenin during axis formation in Xenopus. *J. Cell Biol.* **132**, 1105-1114.

Ferrari, S. L., Traianedes, K., Thorne, M., Lafage-Proust, M. H., Genever, P., Cecchini, M. G., Behar, V., Bisello, A., Chorev, M., Rosenblatt, M. et al. (2000). A role for N-cadherin in the development of the differentiated osteoblastic phenotype. *J. Bone Miner. Res.* **15**, 198-208.

Fischer, L., Boland, G. and Tuan, R. S. (2002). Wnt-3A enhances bone morphogenetic protein-2-mediated chondrogenesis of murine C3H10T1/2 mesenchymal cells. *J. Biol. Chem.* **277**, 30870-30878.

Fujimori, T. and Takeichi, M. (1993). Disruption of epithelial cell-cell adhesion by exogenous expression of a mutated nonfunctional N-cadherin. *Mol. Biol. Cell* **4**, 37-47.

Gumbiner, B. M. (1996). Cell adhesion: the molecular basis of tissue architecture and morphogenesis. *Cell* **84**, 345-357.

Haas, A. R. and Tuan, R. S. (1999). Chondrogenic differentiation of murine C3H10T1/2 multipotential mesenchymal cells: II. Stimulation by bone morphogenetic protein-2 requires modulation of N-cadherin expression and function. *Differentiation* **64**, 77-89.

Hermiston, M. L. and Gordon, J. I. (1995). In vivo analyisis of cadherin

function in the mouse intestinal epithelium: Essential roles in adhesion, maintenance of differentiation, and regulation of programmed cell death. *J. Cell Biol.* **129**, 489-506.

Jilka, R. L., Weinstein, R. S., Takahashi, K., Parfitt, A. M. and Manolagas, S. C. (1996). Linkage of decreased bone mass with impaired osteoblastogenesis in a murine model of accelerated senescence. *J. Clin. Invest.* **97**, 1732-1740.

Kawaguchi, J., Azuma, Y., Hoshi, K., Kii, I., Takeshita, S., Ohta, T., Ozawa, H., Takeichi, M., Chisaka, O. and Kudo, A. (2001a). Targeted disruption of cadherin-11 leads to a reduction in bone density in calvaria and long bone metaphyses. *J. Bone Miner. Res.* **16**, 1265-1271.

Kawaguchi, J., Kii, I., Sugiyama, Y., Takeshita, S. and Kudo, A. (2001b). The transition of cadherin expression in osteoblast differentiation from mesenchymal cells: consistent expression of cadherin-11 in osteoblast lineage. *J. Bone Miner. Res.* **16**, 260-269.

Kintner, C. (1992). Regulation of embryonic cell adhesion by the cadherin cytoplasmic domain. *Cell* **69**, 225-236.

Lai, C.-F., Chaudhary, L., Fausto, A., Halstead, L. R., Ory, D. S., Avioli, L. V. and Cheng, S. L. (2001). Erk is essential for growth, differentiation, integrin expression, and cell function in human osteoblastic cells. *J. Biol. Chem.* **276**, 14443-14450.

Lecanda, F., Warlow, P. M., Sheikh, S., Furlan, F., Steinberg, T. H. and Civitelli, R. (2000). Connexin43 deficiency causes delayed ossification, craniofacial abnormalities, and osteoblast dysfunction. *J. Cell Biol.* **151**, 931-944.

Liu, C. C. and Kalu, D. N. (1990). Human parathyroid hormone-(1-34) prevents bone loss and augments bone formation in sexually mature ovariectomized rats. *J. Bone Miner. Res.* **5**, 973-982.

Marie, P. J. (2002). Role of N-cadherin in bone formation. *J. Cell Physiol.* **190**, 297-305.

Nagafuchi, A. (2001). Molecular architecture of adherens junctions. *Curr. Opin. Cell Biol.* **13**, 600-603.

Nieman, M. T., Kim, J. B., Johnson, K. R. and Wheelock, M. J. (1999). Mechanism of extracellular domain-deleted dominant negative cadherins. *J. Cell Sci.* **112**, 1621-1632.

Okazaki, M., Takeshita, S., Kawai, S., Kikuno, R., Tsujimura, A., Kudo, A. and Amann, E. (1994). Molecular cloning and characterization of OB-cadherin, a new member of cadherin family expressed in osteoblasts. *J. Biol. Chem.* **269**, 12092-12098.

Orsulic, S., Huber, O., Aberle, H., Arnold, S. and Kemler, R. (1999). E-cadherin binding prevents beta-catenin nuclear localization and beta-catenin/LEF-1-mediated transactivation. *J. Cell Sci.* **112**, 1237-1245.

Parfitt, A. M., Drezner, M. K., Glorieux, F. H., Kanis, J. A., Malluche, H., Meunier, P. J., Ott, S. M. and Recker, R. R. (1987). Bone histomorphometry: standardization of nomenclature, symbols, and units. Report of the ASBMR Histomorphometry Nomenclature Committee. *J. Bone Miner. Res.* **2**, 595-610.

Peifer, M. and Polakis, P. (2000). Wnt signaling in oncogenesis and embryogenesis – a look outside the nucleus. *Science* **287**, 1606-1609.

Radice, G. L., Rayburn, H., Matsunami, H., Knudsen, K. A., Takeichi, M. and Hynes, R. O. (1997). Developmental defects in mouse embryos lacking N-cadherin. *Dev. Biol.* **181**, 64-78.

Rawadi, G., Vayssiere, B., Dunn, F., Baron, R. and Roman-Roman, S. (2003). BMP-2 controls alkaline phosphatase expression and osteoblast mineralization by a Wnt autocrine loop. *J. Bone Miner. Res.* **18**, 1842-1853.

Ross, S. E., Hemati, N., Longo, K. A., Bennett, C. N., Lucas, P. C., Erickson, R. L. and MacDougald, O. A. (2000). Inhibition of adipogenesis by Wnt signaling. *Science* **289**, 950-953.

Sadot, E., Simcha, I., Shtutman, M., Ben, Ze'ev, A. and Geiger, B. (1998). Inhibition of beta-catenin-mediated transactivation by cadherin derivatives. *Proc. Natl. Acad. Sci. USA*. **95**, 15339-15344.

Shin, C. S., Lecanda, F., Sheikh, S., Weitzmann, L., Cheng, S. L. and Civitelli, R. (2000). Relative abundance of different cadherins defines differentiation of mesenchymal precursors into osteogenic, myogenic, or adipogenic pathways. *J. Cell. Biochem.* **78**, 566-577.

Takeichi, M. (1995). Morphogenetic roles of classic cadherins. *Curr. Opin. Cell Biol.* **7**, 619-627.

Tuan, R. S. (2003). Cellular signaling in developmental chondrogenesis: N-cadherin, Wnts, and BMP-2. *J. Bone Joint Surg. Am.* **85-A (Suppl. 2)**, 137-141.

Tuli, R., Tuli, S., Nandi, S., Huang, X., Manner, P. A., Hozack, W. J., Danielson, K. G., Hall, D. J. and Tuan, R. S. (2003). Transforming growth factor-beta-mediated chondrogenesis of human mesenchymal progenitor cells involves N-cadherin and mitogen-activated protein kinase and Wnt signaling cross-talk. *J. Biol. Chem.* **278**, 41227-41236.

Zhu, A. J. and Watt, F. M. (1999). β-catenin signalling modulates proliferative potential of human epidermal keratinocytes independently of intercellular adhesion. *Development* **126**, 2285-2298.